FINAL REPORT
U.S. Department of Energy

Calcite Precipitation and Trace Metal Partitioning in Groundwater and the Vadose Zone: Remediation of Strontium-90 and Other Divalent Metals and Radionuclides in Arid Western Environments

Principal Investigator: F. Grant Ferris
Institution: University of Toronto

Project Number: 70206

Grant Number: DE-FG07-99ER15025

Grant Project Officer: Roland F. Hirsch

Project Duration: September 15, 1999 to January 31, 2003

Table of Contents

Executive Summary		ii
1.0	Research Objectives	1
2.0	Methods and Results	3
3.0	Relevance, Impact and Technology Transfer	14
4.0	Project Productivity	15
5.0	Personnel Supported	15
6.0	Publications	15
7.0	Interactions	16
8.0	Transitions and Future Work	16
9.0	Patents	16
10.0	Literature Cited	16

Executive Summary

In situ remediation is an emerging technology that will play an important role in DOE's environmental restoration program, and is an area where enhancement in fundamental understanding will lead to significantly improved cleanup tools. In situ remediation technologies have inherent advantages because they do not require the costly removal, transport, and disposal of contamination. In addition, these technologies minimize worker exposure because contaminated materials are not brought to the surface. Finally, these technologies will minimize the generation of secondary waste streams with their associated treatment and disposal.

A particularly promising in situ remediation technology is bioremediation. For inorganic contaminants such as radionuclides and metals, in situ bioremediation can be used to alter the mobility or reduce the toxicity of radionuclides and metals by changing the valence state of the radionuclides and metals, degrading or producing complexing ligands, or facilitating partitioning on to or off of solid phases. The purpose of the research presented here was to explore microbially facilitated partitioning of metal and radionuclides by their co-precipitation with calcium carbonate. Although this approach is a very attractive cleanup alternative, its practical implementation requires improved scientific understanding of the geochemical and biological mechanisms involved, particularly with respect to rates and mechanisms of microbially facilitated calcite precipitation.

Of interest for this investigation is the in situ manipulation of calcite precipitation by the microbially catalyzed hydrolysis of urea. The production of ammonia during microbial decomposition of urea tends to drive pH upwards, and results in formation of alkaline conditions. When solution concentrations of Ca^{2+} and HCO_3^- are high enough, calcium carbonate precipitation may occur.

A series of water samples collected from four wells tapping the aquifer underlying Eastern Snake River Plain (ESRP) in the vicinity of the Idaho National Engineering and Environmental Laboratory (INEEL) all tested positively for the presence of urea degrading bacteria. Calcite precipitation experiments were conducted with isolated ESRP urea degrading bacteria and *B. pasteurii* (ATCC 11859), a known urea hydrolyzer. In all of the experiments, visible white precipitates developed within the first thirty minutes after inoculation. The identity of the precipitates as calcite was confirmed by X-ray diffraction. Scanning electron micrographs of the solids revealed both spherical and amorphous precipitates, with microbes in close association with the minerals.

The kinetics of calcite precipitation at 10 to 20 ^{o}C was subsequently investigated using an artificial groundwater (AGW) medium based on the aqueous chemistry of the ESRP aquifer. Experimental data was fit using unconstrained nonlinear regression and optimization to determine rate constants and points of critical supersaturation ($S_{critical}$ i.e., calcite nucleation). The highest rates of calcite precipitation (ca. 0.8 mmole L^{-1} day^{-1}) occurred near $S_{critical}$. While unique time course trajectories of dissolved Ca^{2+} concentrations were observed at the different experimental temperatures, the calcite precipitation rates all followed the same asymptotic profile decreasing progressively with saturation state regardless of temperature. This emphasizes the fundamental kinetic dependence of calcite precipitation on saturation state, which connects the otherwise dissimilar temporal patterns of calcite precipitation that evolved under the different temperature and biogeochemical regimes of the experiments.

1.0 Research Objectives

The Department of Energy (DOE) must evaluate or clean up extensive waste problems in the vadose zone and groundwater at federal sites due to years of radionuclide, transuranic and metal disposal. The costs associated with cleanup of DOE lands are estimated to be hundreds of billions of dollars over many decades. In addition, many of the contaminated sites cannot be remediated with existing technology. The development of new technologies will reduce some cleanup costs and make possible other remediation efforts that are currently not feasible due to the nature of the wastes and the complexity of the geologic environments in which the wastes reside. However, the cost-effective development of new technologies requires a sound understanding of the fundamental science upon which these technologies are based.

In situ remediation is an emerging technology that will play an important role in DOE's environmental restoration program and is an area where enhancement in fundamental understanding will lead to significantly improved cleanup tools. In situ remediation technologies have inherent advantages because they do not require the costly removal, transport, and disposal of contamination. In addition, these technologies minimize worker exposure because contaminated materials are not brought to the surface. Finally, these technologies will minimize the generation of secondary waste streams with their associated treatment and disposal.

A particularly promising in situ remediation technology is bioremediation. In situ biological methods of destroying or immobilizing organic wastes in groundwater and the vadose zone are often cited as technologies that can provide significant advantages over conventional means of treating waste. Potential benefits of in situ bioremediation include:

- High biogeochemical specificity for targeted wastes
- Complete degradation of the organic constituents of contaminant mixtures yielding non-toxic metabolic byproducts
- Lower cost than conventional technologies
- Direct contact of the microorganisms with the waste in remote locations of the subsurface and therefore high reaction efficiencies for the desired biogeochemical processes

Many of the same advantages exist for the bioremediation of inorganic contamination such as radionuclides and metals except that biological processes are incapable of destroying the contaminants. However, bioremediation can be used to alter the mobility or reduce the toxicity of radionuclides and metals by

- Changing the valence state of the radionuclides and metals
- Degrading or producing complexing ligands
- Facilitating partitioning on to or off of solid phases (e.g., reductive dissolution of hydrous ferric iron oxides, co-precipitation of sulfides or carbonates)

The purpose of the research presented here was to initiate an investigation on microbially facilitated partitioning of metal and radionuclides by their co-precipitation with calcium carbonate. Although in principle this approach is a very attractive cleanup alternative, its practical implementation requires improved scientific understanding of the geochemical and biological mechanisms involved. Our specific research objectives involved evaluation of the ureolytic capability of indigenous bacteria in groundwater, and elucidation of the rates of microbially facilitated calcite precipitation at 10 to 20°C in an artificial groundwater medium as a

result of the introduction of urea. These objectives were accomplished by conducting integrated laboratory and field research with INEEL collaborators.

Catalysis of Calcium Carbonate Precipitation Rates: Microbial Contributions

Microorganisms contribute to the precipitation of a wide variety of authigenic minerals including oxides, phosphates, carbonates, sulfides, and silicates (Ferris et al. 1987, 1988, 1989, 1995; Konhauser et al. 1993, 1994a, 1994b; Konhauser and Ferris 1996). The mechanisms of microbial mineral precipitation are diverse, but conform generally with chemical equilibrium constraints that regulate nucleation and crystal growth reactions (Stumm and Morgan 1996). Nucleation is the most critical stage for mineral precipitation, and occurs either homogeneously or heterogeneously. In homogeneous reactions, mineral nuclei are formed by the random collision of ions in solution. Heterogeneous nucleation involves formation of crystal nuclei on the surfaces of foreign solids such as microbial cells on mineral surfaces. Once a stable nucleus has formed, crystal growth can proceed spontaneously providing that the solution remains oversaturated. The free energy of crystal nucleation is controlled thermodynamically by the bulk free energy of the solution, and the interfacial free energy of the corresponding solid phase (Stumm and Morgan 1996).

Microbial metabolic activity will often trigger a change in solution chemistry that leads to oversaturation (e.g., production of sulfide by sulfate-reducing bacteria). This can induce mineral precipitation by lowering the bulk free energy term for both homogeneous and heterogeneous nucleation reactions; however, chemically reactive sites on microbial cell surfaces that facilitate metal sorption at the nucleation sites will tend to reduce the interfacial surface tension of the solid phase and decrease the surface area of the nucleus that is in contact with the bulk solution. The result is a reduction in the overall interfacial free energy of the nucleus which is favorable towards heterogeneous nucleation and precipitation.

In laboratory experiments, carbonate precipitates commonly develop on the external surfaces of individual microbial cells (Pentecost and Bauld 1988; Thompson and Ferris 1990; Schultze-Lam and Beveridge 1994). Epicellular carbonate mineral deposition is also common with microorganisms in natural samples (Ferris et al. 1994; Ferris et al. 1995). This pattern of mineralization is generally consistent with the inherent ability of microbial cells to serve as templates for heterogeneous nucleation and crystal growth. The effect is apt to be quite important under disequilibrium conditions (e.g., in groundwater springs where degassing of CO_2 may occur), and in metastable solutions that are oversaturated (Pentecost and Spiro 1990; Stumm and Morgan 1996). Cell surface precipitation contributes further to the development of extremely fine-grain precipitates (i.e., often less than 1.0 mm in diameter), as expected from a lower free energy of nucleation and rapid onset of precipitation (Stumm 1992).

Carbonate minerals are precipitated by several rather divergent groups of microorganisms. These include photoautotrophic cyanobacteria, various anaerobic respiratory bacteria (i.e., sulfate- and iron-reducing bacteria), and bacteria that produce ammonia from the degradation of nitrogen-rich organic matter (Kobluk and Crawford 1988; Thompson and Ferris 1990; Coleman et al. 1993;, Schultze-Lam and Beveridge 1994; Vasconcelos et al. 1995). In each case, the metabolic activities of these different microorganisms contribute directly to the development of highly oversaturated solutions from which carbonate mineral deposition subsequently occurs. Here we on a single process, the production of ammonia.
The production of ammonia during microbial decomposition of nitrogen-rich organic compounds ($R\text{-}NH_2$) tends to drive pH upwards and results in formation of relatively alkaline conditions.

When solution concentrations of Ca^{2+} and HCO_3^- are high enough, calcium carbonate precipitation may take place (Kobluk and Crawford 1988; Dick and Tabatabai 1992).

Specifically, microbial hydrolysis of urea is a potent trigger for calcite precipitation. Bacterial hydrolysis of urea has been used to actively precipitate carbonates as mineral plugging and cementing agents in porous geological media (Ferris and Stehmeier 1992; Ferris et al. 1996). Moreover, because urea is relatively inexpensive, widely available, and degrades to innocuous compounds (carbon dioxide and ammonia) it is an ideal agent for in situ manipulation of subsurface biogeochemical environments. Furthermore, the use of urea to cause an increase in pH is preferable to direct addition of base because the gradual hydrolysis of urea is likely to promote a wider spatial distribution of calcite precipitation in the subsurface formations than the direct addition of base, which would in contrast cause immediate precipitation only in the borehole.

Mineralogy and Trace Metal Uptake of Microbially Precipitated Carbonates

In natural sediments, the most common carbonate minerals are the $CaCO_3$ polymorphs calcite and aragonite. Both will form under the influence of bacterial activity (Kobluk and Crawford 1990), although calcite deposition is more commonly reported (Pentecost and Bauld 1988; Pentecost and Spiro 1990). Ultimately, the type of carbonate mineral phase that is precipitated by bacteria will be controlled by the chemical composition of the aqueous environment in which they are growing. For example, microbial calcite precipitation proceeds in waters containing mostly Ca^{2+}, whereas huntite or hydromagnesite precipitates from Mg^{2+}- rich waters (Thompson and Ferris 1990; Ferris et al. 1994).

Although Sr concentrations of up to 1.0 weight percent are common in aragonite, normal values for Sr substitution in calcites tend to be much lower (Blatt 1982; Deer et al. 1992). This is generally attributed to the availability of more space in the aragonite structure in comparison to that of calcite; however, high precipitation rates sustained by microbial growth have been implicated in the partitioning of up to 1.0 wt. % Sr into calcite (Schultze-Lam and Beveridge 1994; Ferris et al. 1995). Because the larger Sr ion is expected to destabilize the rhombohedral structure of calcite, the effect of small grain size on eliminating long range lattice effects in fresh precipitates is considered to be an important factor in the stability of the Sr-calcite solid solutions (Morse and Bender 1990). In a broader context this implies that solid solution formation involving trace metal species like Sr may actually be significantly enhanced in natural waters, through rapid microbial precipitation of fine-grained carbonate minerals (Ferris et al. 1995).

2.0 Methods and Results

Groundwater Samples

Water samples were collected in September 1998 (USGS-9, -11, and –110A) and February 1999 (TAN 37; screened intervals A and B) from four wells tapping the aquifer underlying ESRP. The ESRP is a semiarid high desert in southeastern Idaho, U.S.A. The stratigraphy of the ESRP is composed of multiple basalt flows with thin interbeds of sedimentary silts and clays, and occasional sand and gravel layers (Colwell and Lehman 1997). Calcite precipitation is an integral reaction of the overall chemistry of the unconfined aquifer (McLing 1994, M. S. thesis, Idaho State University; Wood and Low 1986). Three of the wells sampled for this study were on INEEL property and one just south of the property boundary. Three well volumes were purged prior to sample collection. The sampling depths are shown in Table 1, along with water quality data taken at the time of sampling. Historical water quality data for

ESRP wells generally indicate similar and stable water chemistries across the aquifer in the vicinity of the INEEL. Typical measured concentrations include total organic carbon (TOC) values at < 1 mg/L, Ca^{2+} at ~40 mg/L, Mg^{2+} at ~15 mg/L, Na^{+} at ~15 mg/L, Cl^{-} at ~15 mg/L, SO_4^{2-} at ~30 mg/L, bicarbonate ~160 mg/L, ammonia N at ~0.01 mg/L, and nitrite plus nitrate N at ~1 mg/L (Knobel et al. 1992).

Enrichment and isolation of ureolytic bacteria

Groundwater samples were inoculated into Bacto Urea R Broth and Bacto Urea Agar, both prepared according to the directions in the Difco Manual. Both media contain phenol red, to indicate the pH change associated with ammonia production from urea hydrolysis. A change in color from orange to pink indicates urea hydrolysis. Two ml of each groundwater sample were added to 8 ml of Urea R Broth. For the solid media inoculations, three successive dilutions (0.1 ml into 4.5 ml) of the groundwater samples were made in sterile phosphate buffered saline (PBS; 8.3 mM Na_2HPO_4, 1.6 mM NaH_2PO_4, 145 mM NaCl. pH 7.0) and 0.1 ml aliquots of each dilution were spread onto the urea agar plates. Three replicates were prepared for each different sample and/or dilution. Positive controls were prepared using *Proteus vulgaris* (ATCC 33420) a known ureolytic bacterium, and negative controls were uninoculated. All plates and tubes were incubated aerobically in the dark, without shaking, at room temperature (22 °C).

Plates that were positive for urea-hydrolyzing organisms were used to isolate individual ureolytic species. Individual colonies that exhibited unique colony morphologies were lifted and restreaked onto new urea agar plates, and checked again for ureolytic activity. This process was repeated until colony morphology and microscopic examination indicated isolate purity.

All of the water samples included in this study tested positively for urease activity, in both liquid and solid media. Other groundwater samples collected from elsewhere in eastern Idaho also universally tested positively (data not included in this paper), indicating that urease activity is indeed common in the ESRP aquifer. This finding was not surprising, given that prokaryotic ureases are known to be widespread in the environment, but is welcome in that it confirms that the potential remediation approach will not have to rely on a rare physiological capability.

Calcite precipitation experiments

Cells grown overnight at room temperature in Brain Heart Infusion (BHI) broth supplemented with 20 g/L urea were harvested by centrifugation and washed in sterilized ultrapurified water (UPW). Cell suspensions adjusted to fixed optical densities (OD_{600}) were subsequently prepared in sterile UPW as inocula for the calcite precipitation experiments.

The calcite precipitation medium (CPM) contained 3.0 g/L dehydrated Nutrient Broth (Difco), 25 mM $CaCl_2$, 25 mM $NaHCO_3$, and 333 mM urea (Ferris and Stehmeier 1992; Ferris et al 1996). The medium was filter sterilized, and adjusted to pH 6.5. Two sets of experiments were conducted with *B. pasteurii* (ATCC 11859), a known urea hydrolyzer, at initial OD_{600} values of 0.041 and 0.072. For the ESRP cultures the initial OD_{600} was 0.149. Negative controls were uninoculated. All calcite precipitation experiments were run in triplicate. Cultures were incubated without shaking at room temperature for periods of up to 8 hours.

Dissolved calcium concentrations and pH were measured during the experiments with ion selective electrodes, and ammonium ion concentrations were determined using a commercial spectrophotometric assay (Hach Company, Loveland, CO). At the end of the experiments

precipitated solids were collected by filtration for X-ray diffraction and scanning electron microscopy.

Geochemical equilibrium modeling was performed using the MINEQL program and standard thermodynamic databases provided with the program. The nominal chemical composition of the CPM was used to establish the initial total concentrations of reactive chemical components, and the pCO_2 was fixed at $10^{-3.5}$ atm for a system open to the atmosphere. The total proton concentration was subsequently adjusted to ensure that measured and calculated pH values were equal. Multiple runs were carried out to simulate a titration of the CPM by $(NH_4)_2CO_3$ to mimic the progressive hydrolysis of urea over time by the bacteria. Two sets of computational runs were conducted to examine the impact of both excluding and including calcite in the mass balance calculations of the model. In the former case, model results provided an estimate of the extent of calcite supersaturation expected from progressive addition of $(NH_4)_2CO_3$. The latter case provided predictions for dissolved Ca^{2+} concentrations as calcite precipitation occurred in response to urea hydrolysis.

Following inoculation of the cultures into the CPM the hydrolysis of urea was confirmed by the immediate increase in pH, as well as the production of ammonium. By the end of the eight-hour experiment, the pH in all of the cultures reached similar values (pH 8.3-8.5). The similar pH trends associated with the three ESRP aquifer isolates suggested that they exhibit similar metabolic activities, given the identical initial conditions including OD_{600}.

Experimental flasks inoculated with *B. pasteurii* at higher initial OD_{600} hydrolyzed urea more rapidly than those with the lower initial OD_{600}, as would be expected for an enzyme-mediated reaction. However, the ESRP aquifer isolates, which started with OD_{600} values of 0.149, exhibited ammonium production rates that were more similar to the *B. pasteurii* experiments with initial OD_{600} values of 0.041 than to those with initial OD_{600} values of 0.072. This result suggests that the urease activity in the ESRP aquifer isolates is significantly lower than in the *B. pasteurii*. In all cases however the ammonium concentrations increased linearly with time in the experimental cultures, and because the concentration of urea in the CPM far exceeds reported K_m values for microbial soil urease, pseudo-zero order kinetics was assumed. The ammonium production rate constants for the two *B. pasteurii* experiments were different; however, normalization by the starting OD_{600} of the cultures gives similar ammonium production values, emphasizing that the amount of urease active biomass is critical in determining the overall rate of urea hydrolysis. Similar results have been reported by Nielsen et al. (1998). As noted earlier, the ammonium production rates for the INEEL isolates are markedly lower than for the *B. pasteurii*, indicating the reduced urease activity of the isolates relative to *B. pasteurii*.

In all of the cultures, visible white precipitates developed within the first thirty minutes after inoculation. This was consistent with the thermodynamic calculations, which predicted that while the CPM was initially almost two orders of magnitude under-saturated with respect to calcite, the introduction of less than 1 mM $(NH_4)_2CO_3$ would cause calcite supersaturation. Based on the measured ammonium production rates, this supersaturation likely occurred within the first 12 to 24 minutes of culture growth. The identity of the precipitates as calcite was confirmed by X-ray diffraction. Scanning electron micrographs of the solids revealed both spherical and amorphous morphologies, with microbes in close association with the minerals.

Calcite precipitation in artificial groundwater

An artificial groundwater (AGW) medium was prepared based on the aqueous chemistry of the ESRP groundwater in the vicinity of the Idaho National Engineering and Environmental

Laboratory, Idaho Falls, U.S.A. Major anion and cation concentrations were taken as mean values from historical records (Wood and Low 1986). Specific inorganic chemical constituents of the AGW included KNO_3 (0.0403 mM), $MgSO_4$ (0.448 mM), $CaCl_2$ (1.75 mM), $NaNO_3$ (0.044 mM), $NaHCO_3$ (1.1mM), and $KHCO_3$ (0.0623mM). Organic carbon concentrations in pristine regions of the aquifer are generally less than 0.1 mmole C / L (Wood and Low 1986; McLing 1994), so apart from the addition of 6.0 mM urea (for 20 ^oC experiments) and 25 mM (for 10 and 15 ^oC experiments), no organic carbon was added to the medium.

A pure culture of the Gram-positive, spore-forming, urease positive bacteria *Bacillus pasteurii* **(**ATCC 11859) was used in this investigation to induce calcite precipitation in response to urea hydrolysis (Ferris et al. 1996). The urease deficient species *Bacillus subtilis* 168 was used as a negative control. For experimental work, the bacteria were grown overnight at 30^oC in Brain Heart Infusion broth supplemented with 2% (w/v) of urea and harvested by centrifugation at 6000 rpm for 10 min. After being washed twice in sterile ultra pure water (UPW) by centrifugation, cells were suspended in sterile UPW at an optical density of 0.14 at 600nm. These cell suspensions were subsequently used to inoculate the calcite precipitation experiments.

The AGW medium was initially constituted at double strength to be mixed in equal parts with the washed bacterial suspensions. Because a natural pH near 8.0 leaves SRPA groundwater close to saturation with respect to calcite (McLing 1994), the double strength AGW pH was adjusted to 6.5 with 1.0 N HCl to avoid premature calcite precipitation. Sterilization of the double strength AGW was accomplished by filtration through autoclaved 0.2-µm-pore-size filters. Then 150 mL volumes of were dispensed into autoclaved 500mL glass bottles and inoculated with an equal volume of washed *B. pasteurii* suspension to give a final OD_{600} of 0.07. Separate sets of bottles were inoculated with *B. subtilis,* or amended with sterile UPW, to serve as negative biotic and chemical controls, respectively. All experiments were run in triplicate with static incubation at 20 ^oC, 15 ^oC and 10 ^oC for periods of seven days.

The changes in water chemistry including pH, ammonium, dissolved magnesium, and dissolved calcium were analyzed at one to two day intervals during the experiments. The pH was measured using Corning Model 250 pH meter equipped with a Ross SurFlow combination electrode. Ammonium produced from the hydrolysis of urea by *B. pasteurii* during the experiment was determined by the Nelsser method using a HACH DR-2000 spectrophotometer. Samples after being filtered through 0.2-µm filters were analyzed for changes in dissolved calcium concentrations using a Perkin-Elmer 4000 flame atomic absorption spectrophotometer. Mineral precipitates that formed during incubation were collected at the end of the 7 day experiment from *B. pasteurii* inoculated bottles, and identified by powder X-ray diffraction (XRD) using a Philips XRD system.

Experimental data was fit using unconstrained nonlinear regression and a quasi-Newton optimization routine for parameter estimation (STATISTICA v 5.0). Tests for false local minima were performed by varying the initial parameter estimates. The result with the highest correlation coefficient (i.e., r^2 value) was accepted as the global minimum for the residual variance (i.e., sum of squared residuals) about the regression line. All analyses converged to the same final result, regardless of the initial parameter estimates, as expected for optimal minimization of the deviation between observed experimental and predicted values.

The hydrolysis of urea gives rise to a mechanistic first order rate expression for the rate of urea hydrolysis:

$$\frac{d[urea]}{dt} = -k_{urea}[urea] \qquad [2]$$

Integration yields:

$$[urea]_t = [urea]_0 e^{-k_{urea}t} \qquad [3]$$

where $[urea]_t$ is the concentration of urea remaining at time t, and $[urea]_0$ is the initial urea concentration at $t = 0$. Considering the stoichiometry of the reaction for urea hydrolysis, the amount of urea hydrolyzed at time t is equivalent to one-half of the corresponding dissolved NH_4^+ concentration $[NH_4^+]_t$. Thus, the concentration of urea remaing at t is described by the mass balance expression:

$$[urea]_t = [urea]_0 - \frac{1}{2}[NH_4^+]_t \qquad [4]$$

Combining equations [3] and [4] relates $[NH_4^+]_t$, $[urea]_0$, and k_{urea} in a function permissive to the estimation of urea hydrolysis rate constants (k_{urea}) from experimental measurements of dissolved NH_4^+ concentrations over time:

$$[NH_4^+]_t = 2[urea]_0\left(1 - e^{-k_{urea}t}\right) \qquad [5]$$

The production of ammonium over time from the hydrolysis of urea by *B. pasteurii* at different temperatures in artificial groundwater is shown in Figure 1. At 20 ^oC, most of the urea present at an initial concentration of 6.0 mM was subjected to hydrolysis and consumed within seven days to limit ammonium production stoichiometrically to 12 mM (i.e., 2 moles NH_4^+ produced per mole of urea). Sustained ammonium production occurred at both 15 and 10 ^oC when urea was incorporated into the artificial groundwater at an initial concentration of 25 mM; however, the total amount of ammonium produced over seven days at 15 ^oC. (35 mM) was almost double that which was produced at 10 ^oC (20 mM). In terms of stoichiometric equivalents, approximately two-thirds of the available urea was hydrolyzed at 15 ^oC, whereas only one third was hydrolyzed at 10 ^oC. No ammonium was produced in the abiotic control (i.e., in the absence of bacteria), or in the negative control containing *B. subtilis* (i.e., bacteria incapable of hydrolyzing urea).

Figure 1: Dissolved ammonium concentrations arising over time from the hydrolysis of urea by B. pasteurii at (a) 20 °C, (b) 15 °C, and (c) 10 °C with (d) the corresponding urea hydrolysis rates.

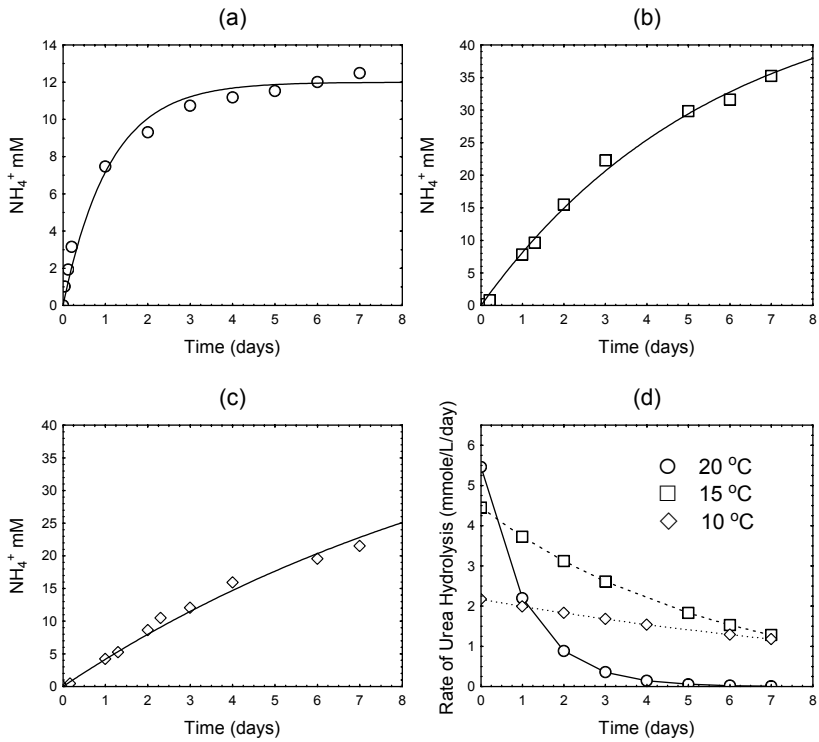

At all temperatures the pH of the AGW medium increased to 9.3 in less than one day. This is consistent with a rapid onset of $NH_4^+ = NH_3 + H^+$ and $HCO_3^- = CO_3^{2-} + H^+$ buffering with pK_a values near 9.3 and 10.4 (over the temperature range of the experiments), respectively (Stumm and Morgan 1996). In the abiotic and *B. subtilis* controls, the pH drifted slowly upwards from 6.5 at the beginning of the experiments to near 7.2 at the end of the experiments.

The saturation state (S) of a solution with respect to calcite is conventionally defined by:

$$S = \frac{\{Ca^{2+}\}\{CO_3^{2-}\}}{K_{so}} \qquad [6]$$

where $\{Ca^{2+}\}$ and $\{CO_3^{2-}\}$ represent the activities of dissolved Ca^{2+} and CO_3^{2-}, repectively, and K_{so} is the equilibrium calcite solubility product. Experimental S values were calculated using the extended Debye-Hückel equation to determine activities of dissolved Ca^{2+} and CO_3^{2-}, with the corresponding K_{so} for each experimental temperature (Stumm and Morgan 1996). Measured dissolved Ca^{2+} concentrations were used for the calculations, whereas CO_3^{2-} concentrations were necessarily derived from speciation of the total dissolved inorganic carbon (C_T) in solution:

$$[CO_3^{2-}] = \alpha_2 C_T \qquad [7]$$

where the mole fraction (α_2) of CO_3^{2-} is (Stumm and Morgan 1996):

$$\alpha_2 = \left(\frac{[H^+]^2}{K_1 K_2} + \frac{[H^+]}{K_2} + 1 \right)^{-1} \qquad [8]$$

The corresponding acidity constants K_1 and K_2 for each experimental temperature are given by Stumm and Morgan (1996), with $[H^+]$ determined from measured pH.

In the experiments, dissolved C_T concentrations changed over time according to the mass balance relationship:

$$C_T = C_{Tinitial} + C_{Turea} - C_{Tcalcite} \qquad [9]$$

where $C_{Tinitial}$ equals the initial dissolved inorganic carbon concentration in the AGW, C_{Turea} is the dissolved inorganic carbon produced from urea hydrolysis (i.e., $[urea]_0 - [urea]_t$ calculated using [4] and [5] after determination of k_{urea}), and $C_{Tcalcite}$ is the dissolved inorganic carbon removed from solution owing to calclite precipitation (i.e, $[Ca^{2+}]_0 - [Ca^{2+}]_t$ calculated using measured dissolved Ca^{2+} concentrations).

Following the onset of calcite precipitation from a saturated solution, the decrease in S with respect to time is anticipated from mass action to be:

$$\frac{dS}{dt} = -k_S \left(\frac{\{Ca^{2+}\}\{CO_3^{2-}\}}{K_{so}} \right) = -k_S S \qquad [10]$$

Integration yields:

$$S_t = S_0 e^{-k_S t} \qquad [11]$$

where S_t is the saturation index at time t, S_0 is the apparent saturation index expected if precipitation started at $t = 0$, and k_S is a first order rate constant. In turn, the rate of Ca^{2+} precipitation in calcite is described by the kinetic relationship (Teng et al. 2000):

$$\frac{d[Ca^{2+}]}{dt} = -k_p(S-1)^2 \qquad [12]$$

Equating [10] and [12] yields:

$$\frac{d[Ca^{2+}]}{dS} = \frac{k_p(S-1)^2}{k_S S} = \frac{k_p S}{k_S} - \frac{2k_p}{k_S} + \frac{k_p}{k_S S} \qquad [13]$$

The integral of [13] becomes:

$$\int_{Ca_{S_i}}^{Ca_S} d[Ca^{2+}] = \frac{k_p}{k_S}\int_{S_{critical}}^{S} SdS - \frac{2k_p}{k_S}\int_{S_{critical}}^{S} dS + \frac{k_p}{k_S}\int_{S_{critical}}^{S} \frac{dS}{S} \qquad [14]$$

Integration yields:

$$[Ca^{2+}]_S = \left(\frac{k_p}{k_S}\right)\left[S\left(\frac{S}{2}-2\right) - S_{critical}\left(\frac{S_{critical}}{2}-2\right) + \ln\left(\frac{S}{S_{critical}}\right)\right] + [Ca^{2+}]_{S_{critical}} \qquad [15]$$

where $S_{critical}$ is the critical supersaturation at which calcite precipitation actually begins, and $[Ca^{2+}]_{Scritical}$ is the dissolved Ca^{2+} concentration at $S_{critical}$, which is equivalent to the initial concentration of dissolved Ca^{2+} at time zero. In order to reduce the parameterization of [15] to estimate $S_{critical}$ and k_p, values for k_S were first determined independently (as described below) using [11].

Dissolved Ca^{2+} concentrations started to decrease in an asymptotic fashion after one day at 20 °C and 15 °C, and two days at 10 °C (Fig. 2a). The progressive loss of Ca^{2+} from solution was accompanied by the development of solid phase precipitates that imparted a faint cloudiness to the otherwise transparent bacterial cultures. Analyses of the precipitates at the end of experiments by X-ray diffraction confirmed that the formation of calcite accounted for the observed depletion of dissolved Ca^{2+} at each of the investigated temperatures.

The most pronounced decreased in dissolved Ca^{2+} concentrations over time came about at 15 °C (Fig. 2a). At 20 °C, the depletion of Ca^{2+} from solution was somewhat less rapid leaving more Ca^{2+} in solution at the end of the experiments than at 15 °C. On the other hand, the delay in Ca^{2+} precipitation observed at 10 °C resulted initially in the highest dissolved Ca^{2+} concentrations; however, once calcite precipitation started Ca^{2+} concentrations declined to at least the same extent as that which occurred at 15 °C and 20 °C. While these trajectories of Ca^{2+} depletion over time do not appear to correlate directly with rates of urea hydrolysis at the different temperatures (Fig. 1d), plots of dissolved Ca^{2+} concentrations as a function of produced ammonium (Fig. 2b) show clearly that calcite precipitation was initiated at similar (i.e., approximately 8.0 mM)

concentrations of ammonium. Considering that the initial concentration of dissolved Ca^{2+} was fixed in the AGW medium, this indicates that calcite precipitation was triggered by approximately the same degree of oversaturation in each of the experiments; i.e., the ratio of the product of dissolved Ca^{2+} and CO_3^{2-} activities (arising from the hydrolysis of urea by *B. pasteurii*) to the temperature dependent calcite solubility product (eqn. 6; Stumm and Morgan 1996).

Figure 2: Dissolved calcium concentrations as a function of (a) time and (b) dissolved ammonium concentrations arising from the hydrolysis of urea by B. pasteurii at 20 °C, 15 °C, and 10 °C. (c) Calculated saturation index (*S*) values as a function of ammonium concentrations for each of the experimental temperatures.

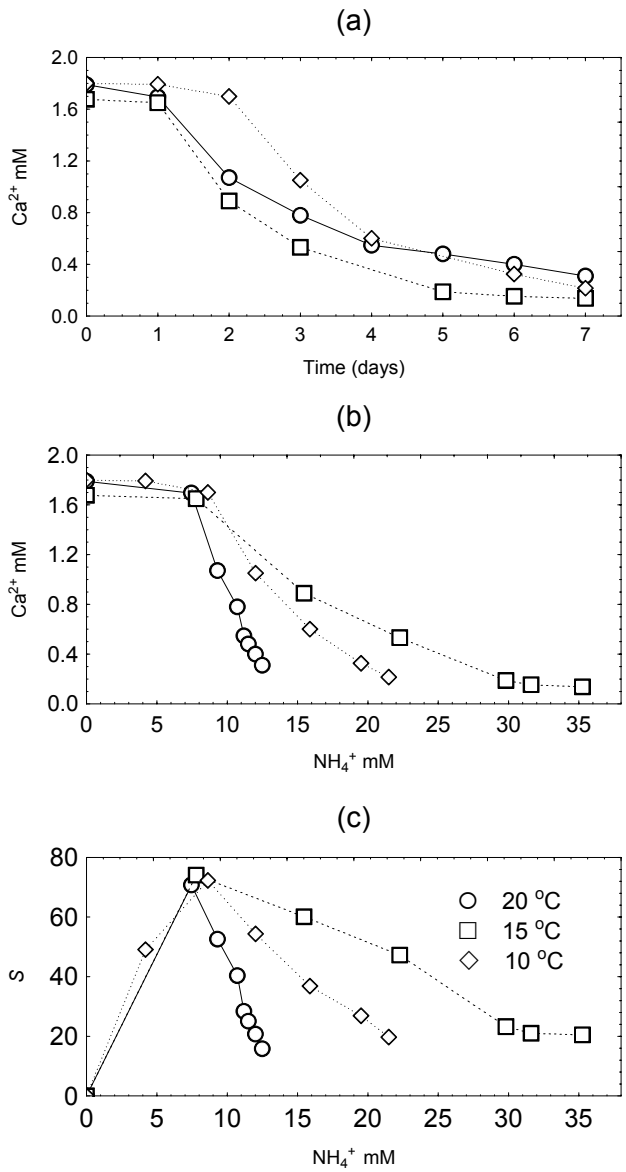

The reason for the temporal displacement of Ca^{2+} precipitation is more precisely evident from plots of the calculated saturation state for the different experiments as a function of ammonium concentrations (Fig. 2c). Initially, saturation states increased rapidly to reach values nearly 80 times greater than the corresponding calcite solubility products (Stumm and Morgan 1996). At the different temperatures, measured ammonium concentrations around 8.0 mM yielded similar peak saturation state values. The subsequent removal of dissolved Ca^{2+} and CO_3^{2-} from solution following the onset of calcite precipitation subsequently sustained a decrease in calculated saturation state values that was most evident at 20 ^oC, and least evident at 15 ^oC. These different trends can be traced to the greater extent of urea hydrolysis and production of CO_3^{2-} at 15^oC in comparison to 10 ^oC and 20^oC (Fig. 1).

The anticipated first order dependence for the decrease in saturation state in response to ongoing calcite precipitation over time (eqn. 11) provided an accurate description (i.e., r^2 values > 0.90) for experimental data acquired following the onset of Ca^{2+} depletion from solution; specifically, one day in the case of 15 ^oC and 20 ^oC, and two days in the case of 10 ^oC (Fig. 3). Rate constants (i.e., k_S values) determined from the nonlinear optimization were similar at all temperatures (Table 1), as expected given that saturation state values were calculated using temperature compensated calcite solubility products (Stumm and Morgan 1996). In contrast, estimates for the apparent critical saturation state required for calcite precipitation at $t = 0$ (i.e., S_0 values) increased as temperature decreased (Table 1). This observation is consistent with the increased temporal displacement witnessed in the onset of calcite precipitation at low temperature (Fig. 2); i.e., despite comparable k_S values a longer period of time was needed to reach S_0 at 10^oC than 15 ^oC or 20 ^oC. In accordance with the estimates for k_S and S_0, the trajectories for calculated rates of change in saturation state at 15^oC and 20 ^oC nearly overlap while a parallel trajectory displaced by one day is followed at 10 ^oC (Fig. 3d).

Table 1: Summary of kinetic parameters for urea hydrolysis (k_{urea}), change in saturation state (k_S), calcite precipitation (k_p), apparent critical saturation (S_0), effective critical saturation (S_{crit}), and delay time for calcite precipitation at different temperatures.

Temperature (^oC)	k_{urea} (day^{-1})	k_S (day^{-1})	k_p (μmoles/L/day)	S_0	S_{crit}	Delay Time (days)
10	0.09	0.27	0.17	121	72	1.89
15	0.18	0.25	0.15	96	76	1.03
20	0.91	0.26	0.16	90	70	0.79

Figure 3: Regression curves from nonlinear optimization analysis for the observed decrease in saturation index (*S*) over time after the onset of calcite precipitation at (a) 20 ^{o}C, (b) 15 ^{o}C, and (c) 10 ^{o}C with (d) the corresponding rates of change in *S*.

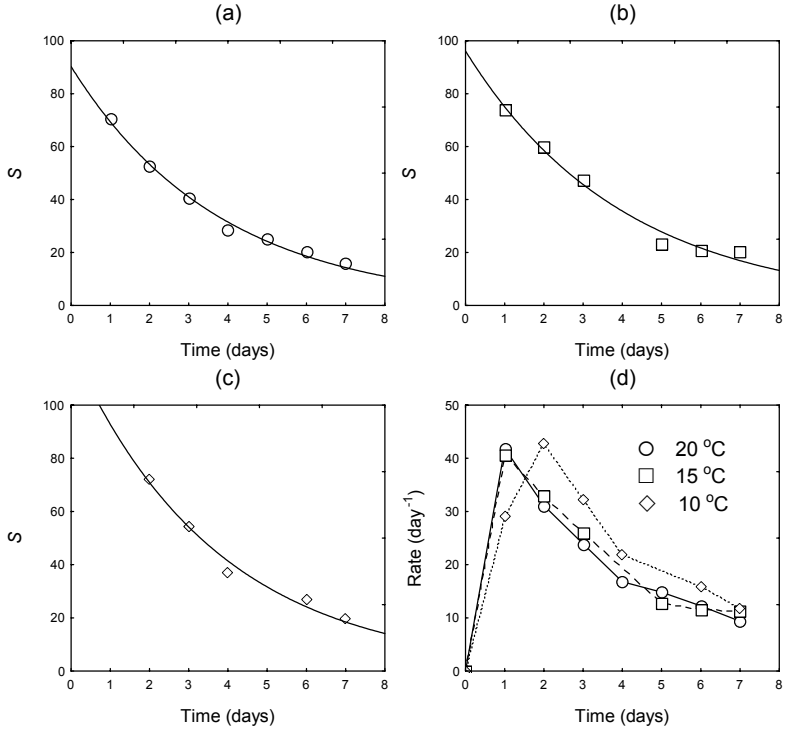

The dissolved Ca^{2+} concentrations measured at each temperature following the onset of calcite precipitation are plotted in Fig. 4 as a function of corresponding saturation state values. Specific rate constants for calcite precipitation (k_p) and effective critical saturation state ($S_{critical}$) derived in accordance with eqn 15 from nonlinear optimization analyses (Table 1) yielded individual curves that explain greater than 90% of the variation in the dissolved Ca^{2+} concentration data (i.e., r^2 values > 0.90). The calcite precipitation rate constants and critical saturation states varied by less than 10 % between the temperatures with mean values of 0.16 $\pm$ 0.01 μmoles L^{-1} day^{-1} and 73 $\pm$ 3, respectively. This apparent independence of k_p and $S_{critical}$ to temperature is in keeping with the temperature dependency imparted by differences in calcite solubility over the temperature range of the experiments. Moreover, the similarity of between estimated $S_{critical}$ values at the different temperatures parallels measurements of dissolved Ca^{2+} and NH_4^+ concentrations (Fig. 2b) which indicate that calcite precipitation was initiated, regardless of temperature, at equivalent concentrations of NH_4^+ (i.e., ca. 8 mM). Substitution of $S_{critical}$ values into eqn 11 permitted further a more precise calculation the delay time for the onset of calcite precipitation in the experiments (Table 1); calculated times of 0.79 (20 ^{o}C), 1.02 (15 ^{o}C), and 1.89 (10 ^{o}C) days match closely the delay period for calcite precipitation observed in the dissolved Ca^{2+} time course data (Fig. 2a).

Figure 4: Dissolved calcium concentrations as a function of saturation index (*S*) at 20 °C, 15 °C, and 10 °C. (d) Calculated calcite precipitation rates as a function of *S* for each of the experimental temperatures

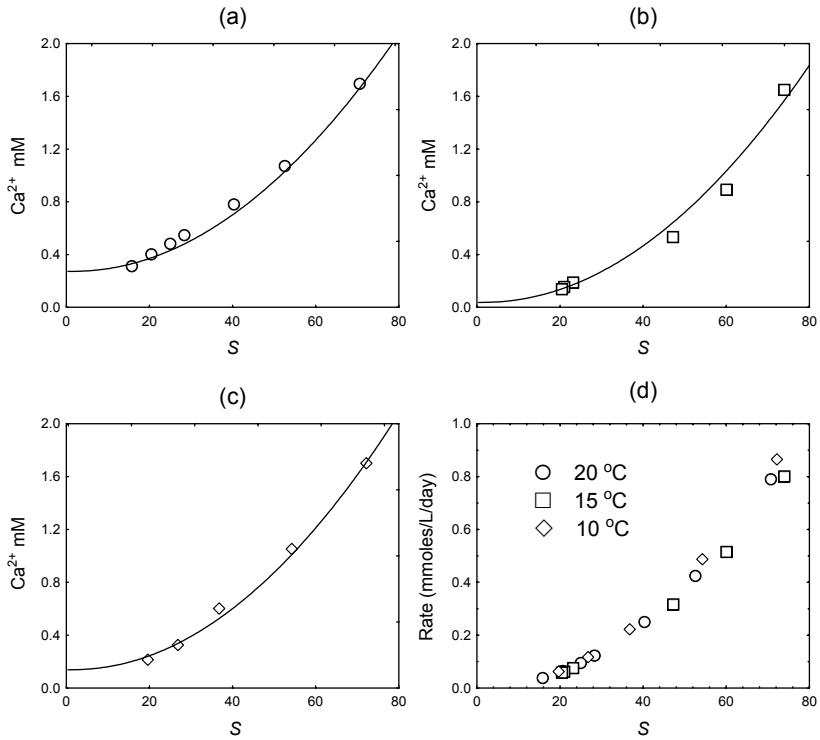

The highest rates of calcite precipitation (ca. 0.8 mmole L^{-1} day^{-1}), calculated by substitution of experimental *S* values and corresponding rate constants (Table 2) into eqn 9, occurred near $S_{critical}$ (Fig. 4d). While unique time course trajectories of dissolved Ca^{2+} concentrations (Fig. 2) and *S* values (Fig. 3) were observed at the different experimental temperatures, the calcite precipitation rates all follow the same asymptotic profile decreasing progressively with *S* regardless of temperature (Fig. 4d). This emphasizes the fundamental kinetic dependence of calcite precipitation on *S*, which connects the otherwise dissimilar temporal patterns of calcite precipitation that evolved under the different temperature and biogeochemical regimes of the experiments.

3.0 Relevance, Impact and Technology Transfer

Demonstration of microbial induced carbonate mineral precipitati, initiated by urea-hydrolysis, indicates that considerable potential exists to realistically adapt this novel immobilization concept to the development of new in situ clean-up strategies for DOE sites where strontium and other metal/radionuclides exist as ubiquitous and often mobile contaminants. These studies have also fundamentally advanced our understanding of how microorganisms influence rates of mineral precipitation reactions in aqueous environments. Moreover, this investigation has enabled further advancement of this concept through a new collaborative EMSP research initiative (Project 87016) at INEEL and the University of Idaho under the direction of R.W. Smith (smithbob@uidaho.edu).

4.0 Project Productivity

This project has accomplished the original goal of developing a better quantitative understanding of microbiological and geochemical controls on carbonate mineral precipitation reactions that are caused by ureolytic bacteria, and has determined key kinetic parameters to assess potential contributions and constraints of these processes for the solid phase capture and immobilization of strontium in the subsurface.

5.0 Personnel Supported

Graduate students

Y. Litwin
R. James

Postdoctoral research associates

Dr. D.S. Smith
Dr. V. Phoenix
Dr. N. Parmar

6.0 Publications

Published in peer-reviewed journals

Fujita, Y., F.G. Ferris, R.D. Lawson, F.S. Colwell, and R.W. Smith. 2000. Calcium carbonate precipitation by ureolytic subsurface bacteria. Geomicrobiology Journal 17: 305-318.

Warren, L.A., P. Maurice, N. Parmar, and F.G. Ferris. 2001. Microbially mediated carbonate precipitation: implications for interpreting calcite preciptation and for solid phase capture of inorganic contaminants. Geomicrobiology J. 18: 93-115.

Published in proceedings

None

Accepted/submitted/in preparation for publication

F.G. Ferris, V. Phoenix, Y. Fujita, and R.W. Smith. Kinetics of Calcite Precipitation Induced by Ureolytic Bacteria at 10 to 20 ^{o}C in Artificial Groundwater. Submitted to *Geochemica Cosmochimca Acta*

Graduate student theses

None

7.0 Interactions

Participation at meetings

Fujita, Y., F.G. Ferris, R.D. Lawson, F.S. Colwell, and R.W. Smith. 2000. Accelerated calcium carbonate precipitation by aquifer microorgansims: a possible in situ remediation technique for radionuclides and metals. American Chemical Society Annual Meeting, Washington, D.C., U.S.A.

Colwell, F.S., R. W. Smith, F. G. Ferris, J. C.Ingram, and A. L. Reysenbach.› Y. Fujita, J. L. Taylor, T.L. Tyler, M. E. Delwiche, and M. M. Cortez. 2002. Calcite Precipitation and Trace Metal Partitioning in Groundwater and the Vadose Zone: Remediation of Strontium-90 and Other Divalent Metals and Radionuclides in Arid Western Environments. U.S. Department of Energy EMSP meeting, Washington, D.C., U.S.A.

Y. Fujita, F. G. Ferris, F. S. Colwell and R. W. Smith. 2000 Microbially Accelerated Calcium Carbonate Precipitation fo rRadionuclide Sequestration: Preliminary Laboratory Studies. Oral presentation at the Northwest/Rocky Mountain Regional Meeting of the American Chemical Society, Idaho Falls, ID.

Y. Fujita, R. D. Lawson, F. G. Ferris, F. S. Colwell, and R. W. Smith. 1999. Microbially Accelerated Calcium Carbonate Precipitation for Radionuclide Sequestration: Preliminary Laboratory Evaluations of Urea-Hydrolyzing Organisms. American Geophysical Union Fall Meeting San Francisco, CA. *EOS* **80**:H31B-06.

8.0 Transitions and Future Work

This investigation has enabled further advancement of this concept through a new collaborative EMSP research initiative (Project 87016) at INEEL and the University of Idaho under the direction of R.W. Smith (smithbob@uidaho.edu): Co-Precipitation of Trace Metals in Groundwater and the Vadose Zone Calcite: *In Situ* Containment and Stabilization of Strontium-90 and Other Divalent Metals and Radionuclides at Arid Western DOE Sites.
.

9.0 Patents

None

10.0 Literature Cited

Blatt, H. 1982. Sedimentary Petrology. W. H. Freeman, San Francisco.

Coleman, M. L., D. B. Hedrick, D. R. Lovley, D. C. White and K. Pye. 1993. Reduction of Fe(III) in Sediments by Sulfate-Reducing Bacteria. Nature 361: 436-438.

Colwell, F., M. E. Delwiche, D. Blackwelder, M. Wilson, R. M. Lehman and T. Uchida. 1999. Microbial Communities from Core Intervals, JAPEX/JNOC/GSC Mallik 2L-38 Gas Hydrate Research Well; In Scientific Results from JAPEX/JNOC/GSC Mallik 2L-38 Gas Hydrate

Research Well, Mackenzie Delta, Northwest Territories, Canada, (ed.) S. R. Dallimore, T. Uchida, and T. S. Collett, Geological Survey of Canada, Bulletin 544.

Colwell, F. S. and R. M. Lehman. 1997. Carbon source utilization profiles for microbial communities from hydrologically distinct zones in a basalt aquifer. Microb. Ecol. 33: 240-251.

Deer, W. S., R. A. Howie and J. Zussman. 1992. An Introduction to the Rock Forming Minerals, 2nd ed., Longman, Hong Kong.

Dick, W. A. and M. A. Tabatabai. 1993. Significance and Potential Uses of Soil Enzymes, p. 95-127, in Soil Microbial Ecology (F. B. Mettings, ed.), Marcel Dekker, New York.

Ferris, F. G., L. G. Stehmeier, A. Kantzas and F. M. Mourits. 1996. Bacteriogenic Mineral Plugging. J. Can. Petrol. Technol. 35: 56-61.

Ferris, F. G., C.M. Fratton, J. P. Gerits, S. Schultze-Lam and B. Sherwood Lollar. 1995. Microbial Precipitation of a Strontium Calcite Phase at a Groundwater Discharge Zone Near Rock Creek, British Columbia, Canada. Geomicrobiol. J. 13: 57-67.

Ferris, F. G., R. G. Wiese and W. S. Fyfe. 1994. Precipitation of Carbonate Minerals by Microorganisms: Implications for Silicate Weathering and the Global Carbon Dioxide Budget. Geomicrobiol. J. 12: 1-13.

Ferris, F. G. and L. G. Stehmeier. 1992. Bacteriogenic Mineral Plugging. U.S. Patent No. 5,143,155.

Ferris, F. G., S. Schultze, T. C. Witten, W. S. Fyfe and T. J. Beveridge. 1989. Metal Interactions with Microbial Biofilms in Acidic and Neutral pH Environments. Appl. Environ. Microbiol. 55: 1249-1257.

Ferris, F. G., W. S. Fyfe and T. J. Beveridge. 1988. Metallic Ion Binding by Bacillus Subtilis: Implications for the Fossilization of Microorganisms. Geology 16: 149-152.

Ferris, F. G., W. S. Fyfe and T. J. Beveridge. 1987. Bacterial as Nucleation Sites for Authigenic Minerals in a Metal-Contaminated Lake Sediment. Chem. Geol. 63: 225-232.

Kobluk, D. R. and D. R. Crawford. 1990. A Modern Hypersaline Organic Mud- and Gypsum-Dominated Basin and Associated Microbialites. Palios 5: 134-148.

Konhauser, K.O. and F.G. Ferris. 1996. Diversity of Iron and Silica Precipitation by Microbial Mats in Hydrothermal Waters, Iceland: Implications for Precambrian Iron Formations. Geology 24: 323-326.

Konhauser, K. O., S. Schultze-Lam, F. G. Ferris, W. S. Fyfe, F. J. Longstaffe and T. J. Beveridge. 1994a. Mineral Precipitation by Epilithic Biofilms in the Speed River, Ontario, Canada. Appl. Environ. Microbiol. 60: 549-553.

Konhauser, K. O., W. S. Fyfe, S. Schultze-Lam, F. G. Ferris and T. J. Beveridge. 1994b. Iron Phosphate Precipitation by Epilithic Microbial Biofilms in Arctic Canada. Can. J. Earth Sci. 31: 1320-1324.

Konhauser, K. O., W. S. Fyfe, F. G. Ferris and T.J. Beveridge. 1993. Metal Sorption and Mineral Precipitation by Bacteria in Two Amazonian River Systems: Rio Solimoes and Rio Negro, Brazil. Geology 21: 1103-1106

McLing, T. L. 1994. The Pre-Anthropogenic Groundwater Evolution at the Idaho National Engineering Laboratory, Idaho. MS Thesis, Idaho State University, Pocatello, ID.

Morse, J. W. and M. L. Bender. 1990. Partition Coefficients in Calcite: Examination of Factors Influencing the Validity of Experimental Results and their Application to Natural Systems. Geochim. Cosmochim. Acta 53: 745-750.

Nielsen T.H., T.A. Bonde and J. Sørensen. 1998. Significance of microbial urea turnover in N cycling of three Danish agricultural soils. *FEMS Microbiol. Ecol.* 25: 147-157.

Pentecost, A. and B. Spiro. 1990. Stable Carbon and Oxygen Isotope Composition of Calcites Associated with Modern Freshwater Cyanobacteria and Algae. Geomicrobiol. J. 8: 17-26.

Pentecost, A. and J. Bauld. 1988. Nucleation of Calcite on the Sheaths of Cyanobacteia Using a Simple Diffusion Cell. Geomicrobiol. J. 6: 129-135.

Schultze-Lam, S. and T. J. Beveridge. 1994. Nucleation of Celestite and Strontianite on a Cyanobacterial S-Layer. Appl. Environ. Microbiol. 60: 447-453.

Stumm, W. and J. J. Morgan. 1996. Aquatic Chemistry, 3rd ed., John Wiley, New York.

Stumm, W. 1992. Chemistry of the Solid-Water Interface, John Wiley, New York.

Teng H.H., P.M.Dove and J.J. De Yoreo. 2000. Kinetics of calcite growth: Surface processes and relationships to macroscopic rate laws. *Geochim. Cosmochim. Acta* 64: 2255-2266.

Vasconcelos, C., J. A. McKenzie, S. Bernasconi, D. Grujic and A. J. Tien. 1995. Microbial Mediation as a Possible Mechanism for Natural Dolomite Formation at Low Temperatures. Nature 377: 220-222.

Wood, W. W. and W. H. Low. 1986. Aqueous Geochemistry and Diagenesis in the Eastern Snake River Plain Aquifer system, Idaho, Geol. Soc. Amer. Bull. 97: 1456-1466.